

Strong-force isospin-symmetry breaking in masses of $N \sim Z$ nuclei

P. Bączyk,¹ J. Dobaczewski,^{1,2,3,4} M. Konieczka,¹ W. Satuła,^{1,4} T. Nakatsukasa,⁵ and K. Sato⁶

¹*Institute of Theoretical Physics, Faculty of Physics,*

University of Warsaw, ul. Pasteura 5, PL-02-093 Warsaw, Poland

²*Department of Physics, University of York, Heslington, York YO10 5DD, United Kingdom*

³*Department of Physics, P.O. Box 35 (YFL), University of Jyväskylä, FI-40014 Jyväskylä, Finland*

⁴*Helsinki Institute of Physics, P.O. Box 64, FI-00014 University of Helsinki, Finland*

⁵*Center for Computational Sciences, University of Tsukuba, Tsukuba 305-8577, Japan*

⁶*Department of Physics, Osaka City University, Osaka 558-8585, Japan*

(Dated: February 2, 2017)

Effects of the isospin-symmetry breaking due to the strong interaction are systematically studied for nuclear masses near the $N = Z$ line, using extended Skyrme energy density functionals (EDFs) with proton-neutron-mixed densities and new terms breaking the isospin symmetry. Two parameters associated with the new terms are determined by fitting mirror and triplet displacement energies (MDEs and TDEs) of isospin multiplets. The new EDFs reproduce the MDEs for $T = \frac{1}{2}$ doublets and $T = 1$ triplets, as well as the staggering of TDE for $T = 1$ triplets. The relative strengths of the obtained isospin-symmetry-breaking terms are consistent with the differences in the NN scattering lengths, a_{nn} , a_{pp} , and a_{np} .

Similarity between the neutron-neutron (nn), proton-proton (pp), and proton-neutron (pn) nuclear forces, commonly known as their charge independence, has been well established experimentally already in 1930's, leading to the concept of isospin symmetry introduced by Heisenberg [1] and Wigner [2]. Since then, the isospin symmetry has been tested and widely used in theoretical modelling of atomic nuclei, with explicit violation by the Coulomb interaction. In addition, the nuclear force also weakly violates the isospin symmetry. There exists firm experimental evidence in the nucleon-nucleon (NN) scattering data that it also contains small charge-dependent (CD) components. The differences in the NN phase shifts indicate that the nn interaction, V_{nn} , is about 1% stronger than the pp interaction, V_{pp} , and that the np interaction, V_{np} , is about 2.5% stronger than the average of V_{nn} and V_{pp} [3]. These are called charge-symmetry breaking (CSB) and charge-independence breaking (CIB), respectively. In this paper, we show that the manifestation of the CSB and CIB in nuclear masses can systematically be accounted for in extended nuclear density functional theory (DFT).

The charge dependence of the nuclear force fundamentally originates from mass and charge differences between u and d quarks. The strong and electromagnetic interactions among these quarks give rise to the mass splitting among the baryonic and mesonic multiplets. The neutron is slightly heavier than the proton. The pions, which are the Goldstone bosons associated with the chiral symmetry breaking and are the primary carriers of the nuclear force at low energy, also have the mass splitting. The CSB mostly originates from the difference in masses of protons and neutrons, leading to the difference in the kinetic energies and influencing the one- and two-boson exchange. On the other hand, the major cause of the CIB is the pion mass splitting. For more details, see

Refs. [3, 4].

The isospin formalism offers a convenient classification of different components of the nuclear force by dividing them into four distinct classes. Class I isoscalar forces are invariant under any rotation in the isospin space. Class II isotensor forces break the charge independence but are invariant under a rotation by π with respect to the y -axis in the isospace preserving therefore the charge symmetry. Class III isovector forces break both the charge independence and the charge symmetry, and are symmetric under interchange of two interacting particles. Finally, forces of class IV break both symmetries and are anti-symmetric under the interchange of two particles. This classification was originally proposed by Henley and Miller [4, 5] and subsequently used in the framework of potential models based on boson-exchange formalism, like CD-Bonn [3] or AV18 [6]. The CSB and CIB were also studied in terms of the chiral effective field theory [7, 8]. So far, the Henley-Miller classification has been rather rarely utilized within the nuclear DFT [9, 10], which is usually based on the charge-independent strong forces.

The most prominent manifestation of the isospin symmetry breaking (ISB) is in the mirror displacement energies (MDEs) defined as the differences between binding energies of mirror nuclei:

$$\text{MDE} = BE(T, T_z = -T) - BE(T, T_z = +T). \quad (1)$$

A systematic study by Nolen and Schiffer [11] showed that the MDEs cannot be reproduced by using models involving Coulomb interaction as the only source of the ISB, see also Refs. [9, 12, 13]. Another source of information on the ISB is the so-called triplet displacement energy (TDE):

$$\begin{aligned} \text{TDE} = & BE(T = 1, T_z = -1) + BE(T = 1, T_z = +1) \\ & - 2BE(T = 1, T_z = 0), \end{aligned} \quad (2)$$

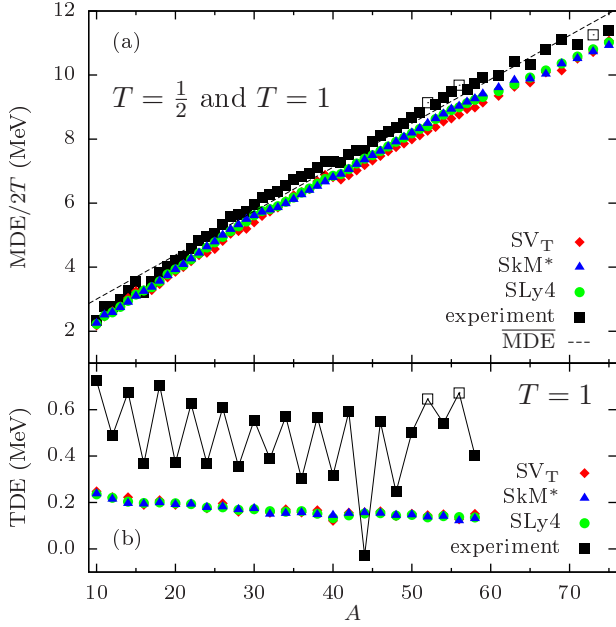


FIG. 1. (Color online) Calculated (no ISB terms) and experimental values of MDEs (a) and TDEs (b). The values of MDEs for triplets are divided by two to fit in the plot. Thin dashed line shows the average linear trend of experimental MDEs in doublets, defined as $\overline{MDE} = 0.137A + 1.63$ (in MeV). Measured values of binding energies were taken from Ref. [24] and the excitation energies of the $T = 1$, $T_z = 0$ states from Ref. [25]. Open squares denote data that depend on masses derived from systematics [24].

which is a measure of the binding-energy curvature within the isospin triplet. The TDE also cannot be reproduced by means of conventional approaches disregarding nuclear CIB forces, see [14]. In these definitions the binding energies are negative ($BE < 0$) and the proton (neutron) has isospin projection of $t_z = -\frac{1}{2}(\frac{1}{2})$.

In Fig. 1 we show MDEs and TDEs calculated fully self-consistently using three different standard Skyrme EDFs; SV_T [15, 16], SkM* [17], and SLy4 [18]. Details of the calculations, performed using code HFODD [19, 20], are presented in the Supplemental Material [21]. In Fig. 1(a), we clearly see that the values of obtained MDEs are systematically lower by about 10% than the experimental ones. Even more spectacular discrepancy appears in Fig. 1(b) for TDEs – their values are underestimated by about a factor of three and the characteristic staggering pattern seen in experiment is entirely absent. It is also very clear that the calculated MDEs and TDEs, which are specific differences of binding energies, are independent of the choice of Skyrme EDF parametrization, that is, of the isospin-invariant part of the EDF.

We aim at comprehensive study of MDEs and TDEs based on extended Skyrme pn -mixed DFT [16, 19, 20] that includes zero-range class II and III forces. We con-

sider the following zero-range interactions of class II and III with two new low-energy coupling constants t_0^{II} and t_0^{III} [26]:

$$\hat{V}^{\text{II}}(i, j) = t_0^{\text{II}} \delta(\mathbf{r}_i - \mathbf{r}_j) \left[3\hat{\tau}_3(i)\hat{\tau}_3(j) - \hat{\tau}(i) \circ \hat{\tau}(j) \right] \quad (3)$$

$$\hat{V}^{\text{III}}(i, j) = t_0^{\text{III}} \delta(\mathbf{r}_i - \mathbf{r}_j) [\hat{\tau}_3(i) + \hat{\tau}_3(j)]. \quad (4)$$

The corresponding contributions to EDF read:

$$\mathcal{H}_{\text{II}} = \frac{1}{2} t_0^{\text{II}} (\rho_n^2 + \rho_p^2 - 2\rho_n\rho_p - 2\rho_{np}\rho_{pn} - \mathbf{s}_n^2 - \mathbf{s}_p^2 + 2\mathbf{s}_n \cdot \mathbf{s}_p + 2\mathbf{s}_{np} \cdot \mathbf{s}_{pn}), \quad (5)$$

$$\mathcal{H}_{\text{III}} = \frac{1}{2} t_0^{\text{III}} (\rho_n^2 - \rho_p^2 - \mathbf{s}_n^2 + \mathbf{s}_p^2), \quad (6)$$

where ρ and \mathbf{s} are scalar and spin (vector) densities, respectively. Inclusion of the spin exchange terms in Eqs. (3) and (4) leads to trivial rescaling of the coupling constants t_0^{II} and t_0^{III} , see [26]. Hence, it can be disregarded.

Contributions of class III force to EDF (6) depend on the standard nn and pp densities and, therefore, can be taken into account within the conventional pn -separable DFT approach [9]. In contrast, contributions of class II force (5) depend explicitly on the mixed densities, ρ_{np} and \mathbf{s}_{np} , and require the use of pn -mixed DFT [27, 28], augmented by the isospin cranking to control the magnitude and direction of the isospin (T, T_z).

We implemented the new terms of the EDF in the code HFODD [19, 20], where the isospin degree of freedom is controlled within the isocranking method [27, 29, 30] – an analogue of the cranking technique that is widely used in high-spin physics. The isocranking method allows us to calculate the entire isospin multiplet, T , by starting from an isospin-aligned state $|T, T_z = T\rangle$ and isocranking it around the y -axis in the isospace. The method can be regarded as an approximate isospin projection. A rigorous treatment of the isospin symmetry within the pn -mixed DFT formalism requires full, three-dimensional isospin projection, which is currently under development.

Physically relevant values of t_0^{II} and t_0^{III} turn out to be fairly small [26], and thus the new terms do not impair the overall agreement of self-consistent results with the standard experimental data. Moreover, calculated MDEs and TDEs depend on t_0^{II} and t_0^{III} almost linearly, and, in addition, MDEs (TDEs) depend very weakly on t_0^{II} (t_0^{III}) [26]. This allows us to use the standard linear regression method, see, e.g. Refs. [31, 32], to independently adjust t_0^{II} and t_0^{III} to experimental values of TDEs and MDEs, respectively. See Supplemental Material [21] for detailed description of the procedure. Coupling constants t_0^{II} and t_0^{III} resulting from such an adjustment are collected in Table I.

In Fig. 2, we show values of MDEs calculated within our extended DFT formalism for the Skyrme SV_T EDF. By subtracting an overall linear trend (as defined in Fig. 1) we are able to show results in extended scale,

TABLE I. Coupling constants t_0^{II} and t_0^{III} and their uncertainties obtained in this work for the Skyrme EDFs SV_T, SkM*, and SLy4.

	SV _T	SkM*	SLy4
t_0^{II} (MeV fm ³)	17 ± 5	25 ± 8	23 ± 7
t_0^{III} (MeV fm ³)	-7.4 ± 1.9	-5.6 ± 1.4	-5.6 ± 1.1

where a detailed comparison with experimental data is possible. In Fig. 3, we show results obtained for TDEs, whereas complementary results obtained for the Skyrme SkM* and SLy4 EDFs are collected in the Supplemental Material [21].

It is gratifying to see that the calculated values of MDEs closely follow the experimental A -dependence, see Fig. 2. It is worth noting that a single coupling constant t_0^{III} reproduces both $T = \frac{1}{2}$ and $T = 1$ MDEs, which confirms conclusions of Ref. [9]. In addition, for the $T = \frac{1}{2}$ MDEs, the SV_T results nicely reproduce (i) changes in experimental trend that occur at $A = 15$ and 39 , (ii) staggering pattern between $A = 15$ and 39 , and (iii) disappearance of staggering between $A = 41$ and 49 (the $f_{7/2}$ nuclei). We note that these features are already present in the SV_T results without the ISB terms, and that adding this terms increases amplitude of the staggering. However, for the SkM* and SLy4 functionals, the staggering of the $T = \frac{1}{2}$ MDEs is less pronounced [21]. We also note that all three functionals correctly describe the A -dependence and lack of staggering of the $T = 1$ MDEs.

It is even more gratifying to see in Fig. 3 that our pn -mixed calculations, with the class-II coupling constant, t_0^{II} , describe absolute values as well as staggering of TDEs very well, whereas results obtained without ISB terms give too small values and show no staggering. Good agreement obtained for the MDEs and TDEs shows that the role and magnitude of the ISB terms are now firmly established.

It is very instructive to look at ten outliers which were excluded from the fitting procedure. They are shown by open symbols in Figs. 2 and 3. (i) There are five outliers that depend on masses of ^{52}Co , ^{56}Cu , and ^{73}Rb , which clearly deviate from the calculated trends for MDEs and TDEs. These masses were not directly measured but derived from systematics [24]. (ii) There are two outliers that depend on the mass of ^{44}V , whose ground-state measurement may be contaminated by an unresolved isomer [33–35]. (iii) Large differences between experimental and calculated values are found in MDE for $A = 16$, 67 and 69 . Inclusion of these data in the fitting procedure would significantly increase the uncertainty of adjusted coupling constants. The former two, (i) and (ii), call for improving experimental values, whereas the last one (iii) may be a result of structural effects not included in our model.

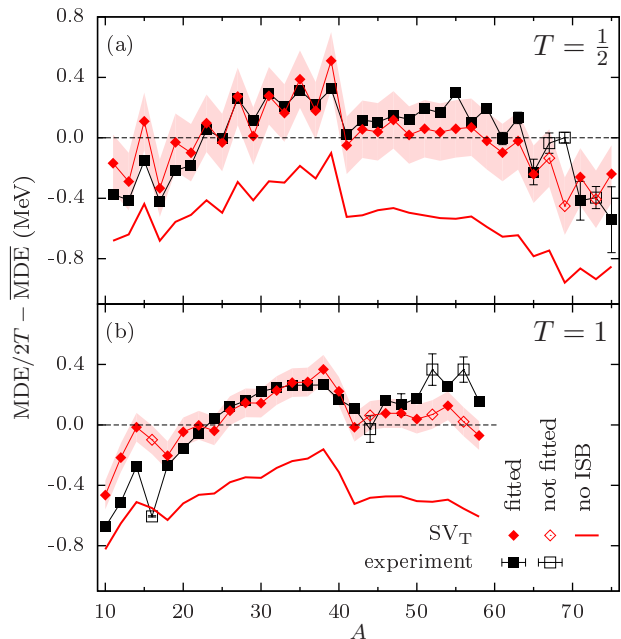


FIG. 2. (Color online) Calculated and experimental values of MDEs for the $T = \frac{1}{2}$ (a) and $T = 1$ (b) mirror nuclei, shown with respect to the average linear trend defined in Fig. 1. Calculations were performed for functional SV_T with the ISB terms added. Shaded bands show theoretical uncertainties. Experimental error bars are shown only when they are larger than the corresponding symbols. Full (open) symbols denote data points included in (excluded from) the fitting procedure.

Having at hand a model with ISB strong interactions with fitted parameters we can calculate MDEs for more massive multiplets and make predictions on binding energies of neutron-deficient ($T_z = -T$) nuclei. In particular, in Table II we present predictions of mass excesses of ^{52}Co , ^{56}Cu , and ^{73}Rb , whose masses were in AME12 [24] derived from systematics, and ^{44}V , whose

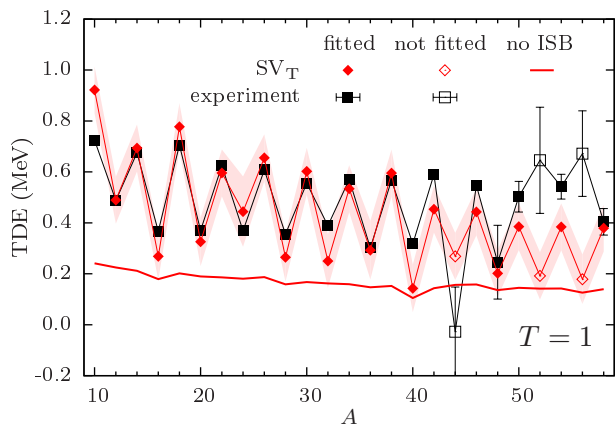


FIG. 3. (Color online) Same as in Fig. 2 but for the $T = 1$ TDEs with no linear trend subtracted.

TABLE II. Mass excesses of ^{52}Co , ^{56}Cu , ^{73}Rb , and ^{44}V obtained in this work and compared with those of AME12 [24]. Our predictions were calculated as weighted averages of values obtained from MDEs and TDEs for all three used Skyrme parametrizations. The AME12 values derived from systematics are labelled with symbol #.

Nucleus	Mass excess (keV)	
	This work	AME12 [24]
^{52}Co	-34450(50)	-33990(200)#
^{56}Cu	-38720(50)	-38240(200)#
^{73}Rb	-46100(80)	-46080(100)#
^{44}V	-23770(50)	-24120(180)

ground-state mass measurement is uncertain. Recently, the mass excess of ^{52}Co was measured as $-34361(8)$ [36] or $-34331.6(66)$ keV [37]. These values are in fair agreement with our prediction (1.8 or 2.4σ difference with respect to our estimated theoretical uncertainty), even though the difference between them is still far beyond the estimated (much smaller) experimental uncertainties.

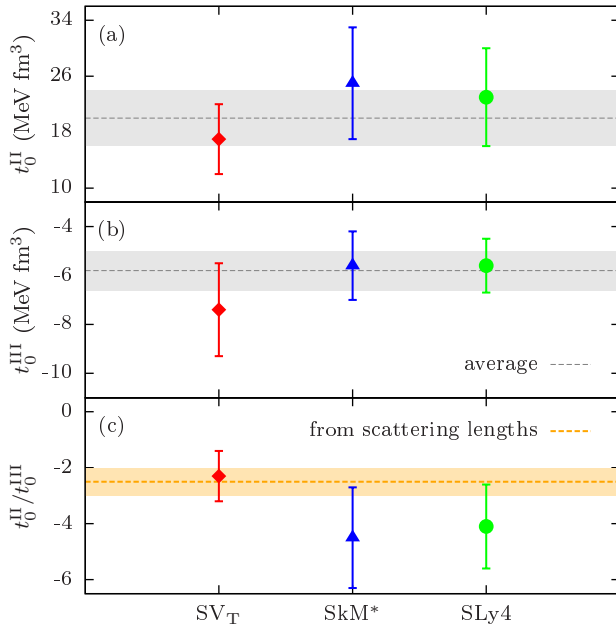


FIG. 4. (Color online) Coupling constants t_0^{II} (a) and t_0^{III} (b), together with their average values and uncertainties. Panel (c) shows ratios of coupling constants $t_0^{\text{II}}/t_0^{\text{III}}$ compared with the value of Eq. (7).

Assuming that the extracted CSB and CIB effects are, predominantly, due to the ISB in the 1S_0 channel we can relate ratio $t_0^{\text{II}}/t_0^{\text{III}}$ to the experimental scattering lengths. The reasoning follows the work of Suzuki *et al.* [10], which assumed a proportionality between the strengths of CSB and CIB forces and the corresponding scattering lengths [?], that is, $V_{\text{CSB}} \propto \Delta a_{\text{CSB}} = a_{pp} - a_{nn}$ and $V_{\text{CIB}} \propto \Delta a_{\text{CIB}} = \frac{1}{2}(a_{pp} + a_{nn}) - a_{np}$,

which, in our case, is equivalent to $t_0^{\text{II}} \propto -\frac{1}{2}\Delta a_{\text{CSB}}$ and $t_0^{\text{III}} \propto \frac{1}{3}\Delta a_{\text{CIB}}$. Assuming further that the proportionality constant is the same, and taking for the experimental values $\Delta a_{\text{CSB}} = 1.5 \pm 0.3$ fm and $\Delta a_{\text{CIB}} = 5.7 \pm 0.3$ fm [?], one gets:

$$\frac{t_0^{\text{II}}}{t_0^{\text{III}}} = -\frac{2}{3} \frac{\Delta a_{\text{CIB}}}{\Delta a_{\text{CSB}}} = -2.5 \pm 0.5. \quad (7)$$

From the values of coupling constants given in Table I, we obtain their ratios as $t_0^{\text{II}}/t_0^{\text{III}} = -2.3 \pm 0.9$, -4.5 ± 1.8 , and -4.1 ± 1.5 for the SV_T, SkM*, and SLy4 EDFs, respectively. Fig. 4 summarizes these values in comparison with the estimate in Eq. (7). As we can see, the values determined by our analysis of masses of $N \simeq Z$ nuclei with $10 \leq A \leq 75$ agree very well with estimates based on properties of the NN forces deduced from the NN scattering experiments.

In summary, we showed that the pn -mixed DFT with added two new terms related to the ISB interactions of class II and III is able to systematically reproduce observed MDEs and TDEs of $T = \frac{1}{2}$ and $T = 1$ multiplets. Adjusting only two coupling constants t_0^{II} and t_0^{III} , we reproduced not only the magnitudes of the MDE and TDE but also their characteristic staggering patterns. The obtained values of t_0^{II} and t_0^{III} turn out to agree with the NN ISB interactions (NN scattering lengths) in the 1S_0 channel. We predicted mass excesses of ^{52}Co , ^{56}Cu , ^{73}Rb , and ^{44}V , and for ^{52}Co we obtained fair agreement with the recently measured values [36, 37]. To better pin down the ISB effects, accurate mass measurements of the other three nuclei are very much called for.

This work was supported in part by the Polish National Science Center under Contract Nos. 2014/15/N/ST2/03454 and 2015/17/N/ST2/04025, by the Academy of Finland and University of Jyväskylä within the FIDIPRO program, by Interdisciplinary Computational Science Program in CCS, University of Tsukuba, and by ImPACT Program of Council for Science, Technology and Innovation (Cabinet Office, Government of Japan). We acknowledge the CIŚ Świerk Computing Center, Poland, and the CSC-IT Center for Science Ltd., Finland, for the allocation of computational resources.

-
- [1] W. Heisenberg, Z. Phys. **77**, 1 (1932).
 - [2] E. Wigner, Phys. Rev. **51**, 106 (1937).
 - [3] R. Machleidt, Phys. Rev. C **63**, 024001 (2001).
 - [4] G. A. Miller and W. H. T. van Oers, *Symmetries and Fundamental Interactions in Nuclei*, edited by W. C. Haxton and E. M. Henley (World Scientific, 1995).
 - [5] E. M. Henley and G. A. Miller, *Mesons in Nuclei*, edited by M. Rho and D. H. Wilkinson (North Holland, 1979).
 - [6] R. B. Wiringa, S. Pastore, S. C. Pieper, and G. A. Miller, Phys. Rev. C **88**, 044333 (2013).

- [7] M. Walzl, U.-G. Meiner, and E. Epelbaum, *Nuclear Physics A* **693**, 663 (2001).
- [8] E. Epelbaum, H.-W. Hammer, and U.-G. Meißner, *Rev. Mod. Phys.* **81**, 1773 (2009).
- [9] B. A. Brown, W. A. Richter, and R. Lindsay, *Physics Letters B* **483**, 49 (2000).
- [10] T. Suzuki, H. Sagawa, and N. Van Giai, *Phys. Rev. C* **47**, R1360 (1993).
- [11] J. A. Nolen, Jr and J. P. Schiffer, *Ann. Rev. Nucl. Sci.* **19**, 471 (1969).
- [12] K. Kaneko, Y. Sun, T. Mizusaki, and S. Tazaki, *Phys. Rev. Lett.* **110**, 172505 (2013).
- [13] G. Colò, H. Sagawa, N. Van Giai, P. F. Bortignon, and T. Suzuki, *Phys. Rev. C* **57**, 3049 (1998).
- [14] W. Satuła, J. Dobaczewski, M. Konieczka, and W. Nazarewicz, *Acta Phys. Pol. B* **45**, 167 (2014).
- [15] M. Beiner, H. Flocard, N. Van Giai, and P. Quentin, *Nucl. Phys. A* **238**, 29 (1975).
- [16] W. Satuła, J. Dobaczewski, W. Nazarewicz, and M. Rafalski, *Phys. Rev. Lett.* **106**, 132502 (2011).
- [17] J. Bartel, P. Quentin, M. Brack, C. Guet, and H.-B. Håkansson, *Nucl. Phys. A* **386**, 79 (1982).
- [18] E. Chabanat, P. Bonche, P. Haensel, J. Meyer, and R. Schaeffer, *Nucl. Phys. A* **635**, 231 (1998).
- [19] N. Schunck, J. Dobaczewski, J. McDonnell, W. Satuła, J. Sheikh, A. Staszczak, M. Stoitsov, and P. Toivanen, *Comput. Phys. Comm.* **183**, 166 (2012).
- [20] N. Schunck, J. Dobaczewski, W. Satuła, P. Bączyk, J. Dudek, Y. Gao, M. Konieczka, K. Sato, Y. Shi, X. Wang, and T. Werner, *arXiv:1612.05314 [nucl-th]*.
- [21] See Supplemental Material at [URL will be inserted by publisher], which includes Refs. [22, 23], for details of the calculations performed using code HFODD, description of the fitting procedure, and results obtained for the Skyrme SkM* and SLy4 EDFs.
- [22] P. Bączyk, J. Dobaczewski, M. Konieczka, T. Nakatsukasa, K. Sato, and W. Satuła, *arXiv:1611.01392 [nucl-th]*.
- [23] W. Satuła, J. Dobaczewski, W. Nazarewicz, and T. Werner, *Phys. Rev. C* **86**, 054316 (2012).
- [24] M. Wang, G. Audi, A. H. Wapstra, F. G. Kondev, M. MacCormick, X. Xu, and B. Pfeiffer, *Chin. Phys. C* **36**, 1603 (2012).
- [25] Evaluated Nuclear Structure Data File, <http://www.nndc.bnl.gov/ensdf/>.
- [26] P. Bączyk, J. Dobaczewski, M. Konieczka, and W. Satuła, *Acta Phys. Pol. B Proc. Supp.* **8**, 539 (2016).
- [27] K. Sato, J. Dobaczewski, T. Nakatsukasa, and W. Satuła, *Phys. Rev. C* **88**, 061301(R) (2013).
- [28] J. A. Sheikh, N. Hinohara, J. Dobaczewski, T. Nakatsukasa, W. Nazarewicz, and K. Sato, *Phys. Rev. C* **89**, 054317 (2014).
- [29] W. Satuła and R. Wyss, *Phys. Rev. Lett.* **86**, 4488 (2001).
- [30] W. Satuła and R. Wyss, *Phys. Rev. Lett.* **87**, 052504 (2001).
- [31] J. Toivanen, J. Dobaczewski, M. Kortelainen, and K. Mizuyama, *Phys. Rev. C* **78**, 034306 (2008).
- [32] J. Dobaczewski, W. Nazarewicz, and P.-G. Reinhard, *J. Phys. G: Nucl. Part. Phys.* **41**, 074001 (2014).
- [33] Y. Fujita, T. Adachi, H. Fujita, A. Algora, B. Blank, M. Csatlós, J. M. Deaven, E. Estevez-Aguado, E. Ganioglu, C. J. Guess, J. Gulyás, K. Hatanaka, K. Hirota, M. Honma, D. Ishikawa, A. Krasznahorkay, H. Matsubara, R. Meharchand, F. Molina, H. Okamura, H. J. Ong, T. Otsuka, G. Perdikakis, B. Rubio, C. Scholl, Y. Shimbara, E. J. Stephenson, G. Susoy, T. Suzuki, A. Tamii, J. H. Thies, R. G. T. Zegers, and J. Zenihiro, *Phys. Rev. C* **88**, 014308 (2013).
- [34] M. MacCormick and G. Audi, *Nuclear Physics A* **925**, 61 (2014).
- [35] X. Tu, Y. Litvinov, K. Blaum, B. Mei, B. Sun, Y. Sun, M. Wang, H. Xu, and Y. Zhang, *Nuclear Physics A* **945**, 89 (2016).
- [36] X. Xu, P. Zhang, P. Shuai, R. J. Chen, X. L. Yan, Y. H. Zhang, M. Wang, Y. A. Litvinov, H. S. Xu, T. Bao, X. C. Chen, H. Chen, C. Y. Fu, S. Kubono, Y. H. Lam, D. W. Liu, R. S. Mao, X. W. Ma, M. Z. Sun, X. L. Tu, Y. M. Xing, J. C. Yang, Y. J. Yuan, Q. Zeng, X. Zhou, X. H. Zhou, W. L. Zhan, S. Litvinov, K. Blaum, G. Audi, T. Uesaka, Y. Yamaguchi, T. Yamaguchi, A. Ozawa, B. H. Sun, Y. Sun, A. C. Dai, and F. R. Xu, *Phys. Rev. Lett.* **117**, 182503 (2016).
- [37] D. A. Nesterenko, A. Kankainen, L. Canete, M. Block, D. Cox, T. Eronen, C. Fahlander, U. Forsberg, J. Gerl, P. Golubev, J. Hakala, A. Jokinen, V. Kolhinen, J. Koponen, N. Lalović, C. Lorenz, I. D. Moore, P. Papadakis, J. Reinikainen, S. Rinta-Anttila, D. Rudolph, L. G. Sarmiento, A. Voss, and J. Äystö, *arXiv:1701.04069*.
- [38] G. Miller, B. Nefkens, and I. I. laus, *Physics Reports* **194**, 1 (1990).

Supplemental material for: Strong-force isospin-symmetry breaking in masses of $N \sim Z$ nuclei

P. Bączyk,¹ J. Dobaczewski,^{1,2,3,4} M. Konieczka,¹ W. Satuła,^{1,4} T. Nakatsukasa,⁵ and K. Sato⁶

¹*Institute of Theoretical Physics, Faculty of Physics,
University of Warsaw, ul. Pasteura 5, PL-02-093 Warsaw, Poland*

²*Department of Physics, University of York, Heslington, York YO10 5DD, United Kingdom*

³*Department of Physics, P.O. Box 35 (YFL), University of Jyväskylä, FI-40014 Jyväskylä, Finland*

⁴*Helsinki Institute of Physics, P.O. Box 64, FI-00014 University of Helsinki, Finland*

⁵*Center for Computational Sciences, University of Tsukuba, Tsukuba 305-8577, Japan*

⁶*Department of Physics, Osaka City University, Osaka 558-8585, Japan*

(Dated: February 2, 2017)

This Supplemental Material explains technical aspects of the method presented in the Letter and provides numerical results that complement the results published therein. We start by providing the reader with details concerning the choice of the basis size. Next, we discuss the subtleties related to the fitting procedure of the two new coupling constants. Finally, we present results obtained for the MDEs and TDEs with the SkM* [1] and SLy4 [2] Skyrme functionals that mirror those for SV_T [3, 4], which were presented in the Letter.

I. CHOICE OF THE BASIS SIZE

The code HFODD [5, 6] used in this work solves the Hartree-Fock (HF) equations in the Cartesian harmonic oscillator (HO) basis. In this work, we use the spherical HO basis whose size is determined by the number of shells, N_0 , taken into account. The numerical stability with respect to N_0 was tested in details in Ref. [7]. It turned out that the optimum choice of number of HO shells (in terms of the trade-off between precision and computing time) is $N_0 = 10$ for light nuclei ($10 \leq A \leq 30$), $N_0 = 12$ for medium-mass nuclei ($31 \leq A \leq 56$) and $N_0 = 14$ for heavier nuclei ($A \geq 57$). In the Letter, we followed these guidelines with exception of the $A = 58$ triplet, which was calculated with $N_0 = 12$ to maintain consistency with other triplets.

II. ADJUSTMENT OF THE MODEL COUPLING CONSTANTS

Results of fit of the model coupling constants t_0^{II} and t_0^{III} , together with essential elements of the fitting procedure, are given in the Letter. In the following subsections we provide further details concerning the methodology used. In particular, we discuss arguments justifying the splitting of the two-dimensional (2D) fit into two one-dimensional (1D) fits. We also discuss and quantify the sources of potential errors and uncertainties.

A. Selecting HF solutions used for fitting

Calculations of MDEs and TDEs involve ground-state energies in even-even, odd- A , and odd-odd nuclei. In the even-even $A = 4n+2$ triplets, the HF solutions representing the 0^+ ground states are unambiguously defined by filling the Kramers-degenerated levels from the bottom of the potential well up to the Fermi energy. However, in the odd- A $T = \frac{1}{2}$ doublets and $A = 4n$ $T = 1$ triplets, the HF solutions representing ground states are not uniquely defined. The ambiguity is related to the orientation of a current generated by unpaired nucleon(s) with respect to the nuclear shape, which gives rise, in triaxial nuclei, to three different solutions that have angular momenta oriented along the intermediate (X), short (Y), and long (Z) axes of the nuclear shape [8]. No tilted-axis solutions were found. In $A = 4n$ $|T = 1, T_z = \pm 1\rangle$ states, one should consider, additionally, the aligned $|\nu \otimes \pi\rangle$ (or $|\bar{\nu} \otimes \bar{\pi}\rangle$) and anti-aligned $|\nu \otimes \bar{\pi}\rangle$ (or $|\bar{\nu} \otimes \pi\rangle$) arrangements of the valence neutron (ν) and proton (π). Let us mention that both the orientation and alignment ambiguities are related to the time-odd parts of the functional, which are very poorly constrained.

To test dependence of MDEs or TDEs on the orientation and alignment of the HF solutions, for SV_T we performed the complete set of calculations. We found that theoretical MDEs in both $T = \frac{1}{2}$ and $T = 1$ multiplets weakly depend on both the orientation and alignment. The corresponding uncertainty turned out to be of the order of 10 keV, and thus in the total uncertainty budget of MDE, it could be neglected. Accordingly, we performed calculations of MDEs using only the lowest-energy HF solutions obtained for any given Skyrme functional.

At variance with the results obtained for MDEs, for TDEs the influence of the orientations of the HF solutions turned out to be significant. Hence, in this case we computed TDEs for each of the three orientations separately, and then we averaged out the obtained results. The corresponding standard deviations associated with the averaging procedure was carried over to the total uncertainty budget. For SV_T, the fitting procedure was done separately for the aligned and anti-aligned configurations. These two sets of solutions led to similar values of t_0^{II} coupling constant, and to similar predictions

for the TDEs. Based on this observation, we decided to perform the calculations for other parametrizations only with aligned solutions which are much easier to converge at the HF level.

Unfortunately, for certain values of A , we were unable to find solutions for all orientations. The missing solutions were: for SV_T , $A = 12$ and 16 ; for SkM^* , $A = 12, 16, 20, 24, 28, 32, 40, 44$, and 52 ; for $SLy4$, $A = 12, 16, 28, 32, 40$, and 52 . Furthermore, for SkM^* and $SLy4$, solutions for $A = 30$ and 36 triplets turned out to be spherically symmetric, which led to unexpectedly large values of TDE. Therefore, those points were excluded from fitting.

B. The fitting strategy

Our model has two free coupling constants, t_0^{II} and t_0^{III} (see Eqs. (5) and (6) of the paper), which are adjusted to reproduce all available data on MDEs and TDEs in isospin doublets and triplets. The most general strategy would be to perform the 2D fit to the data, that is, to fit both coupling constants simultaneously. However, the 2D procedure is very costly computationally, as it requires both the doublets and triplets to be calculated in the pn -mixing formalism. Fortunately, coupling constants t_0^{II} and t_0^{III} are to a large extent independent of one another. Indeed, test calculations without Coulomb, performed in Ref. [9], clearly indicate that coupling constant t_0^{II} does not affect MDEs. The same calculations showed that the influence of coupling constant t_0^{III} on TDEs is also very weak, and comes mostly from a subtle modification of the HF solution due to the self-consistency of solutions. This property allows us to replace the rigorous 2D procedure by two constitutive 1D fits.

To reduce a possible discrepancy between the full 2D fit and our simplified fitting procedure, we first performed the adjustment of t_0^{III} coupling constant to MDEs. In the next step, for the physical value of t_0^{III} obtained previously, we performed the adjustment of t_0^{II} to TDEs. The adopted strategy allowed us to compute the doublets within the standard pn -separable formalism, thus reducing the computational effort considerably. Moreover, the calculations showed almost perfect linearity of MDEs (TDEs) as functions of t_0^{III} (t_0^{II}). For typical calculations, this fact is illustrated in Figs. 5 and 6. Such linearity, in turn, allowed us to compute derivatives of MDEs and TDEs over the coupling constants by using only two values of the coupling constants. Actually, to verify the linearity and to double-check the obtained results, we used three or four values. The errors introduced by the assumed linearity turned out to be negligible.

C. Penalty function and minimization procedure

The 1D fitting was based on the χ^2 minimization procedure described in Ref. [10]. We defined the penalty

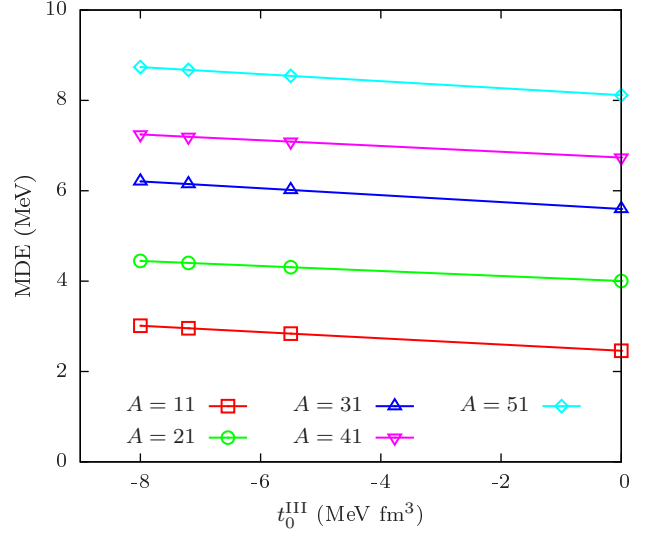


FIG. 5. (Color online) MDEs of $T = \frac{1}{2}$ doublets calculated for different values of t_0^{III} ($t_0^{II} = 0$) and for SV_T . Calculated points are connected with line segments that are almost perfectly parallel to one another.

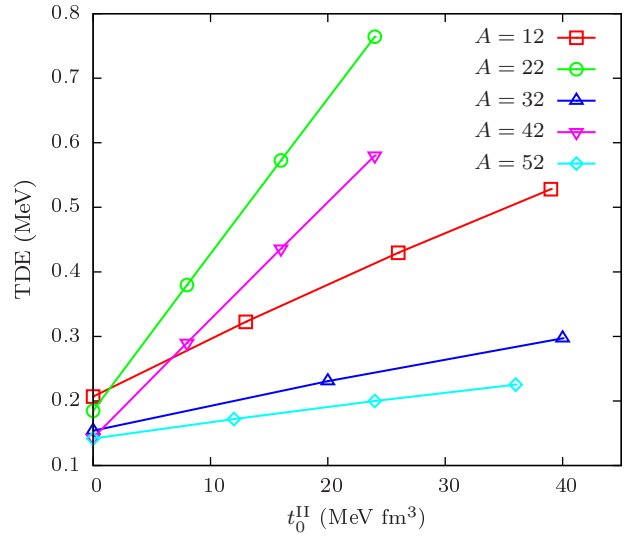


FIG. 6. (Color online) TDEs of $T = 1$ triplets calculated for different values of t_0^{II} ($t_0^{III} = -7.4 \text{ MeV fm}^3$) and for SV_T . Calculated points are connected with line segments.

function χ^2 in the following way:

$$\chi^2(t_0) = \sum_{i=1}^{N_d} \frac{(\text{DE}_i(t_0) - \text{DE}_i^{\text{exp}})^2}{\Delta \text{DE}_i^2}, \quad (8)$$

where t_0 represents the actual coupling constants, t_0^{II} or t_0^{III} , used in the 1D fitting, N_d is the number of experimental data points, $\text{DE}_i(t_0)$ represents the displacement energies, MDEs or TDEs, calculated for a given value of coupling constant t_0 , and DE_i^{exp} are the experimental values of the displacement energies. The denominator,

$\Delta \text{DE}_i^2 = (\Delta \text{DE}_i^{\text{exp}})^2 + (\Delta \text{DE}_i^{\text{the}})^2 + \Delta \text{DE}_{\text{mod}}^2$, is the error comprising three components:

- $\Delta \text{DE}_i^{\text{exp}}$ is the experimental error evaluated from errors of the binding and excitation energies as given in Refs. [11, 12],
- $\Delta \text{DE}_i^{\text{the}}$ is the theoretical uncertainty related to the averaging over orientations as described above,
- $\Delta \text{DE}_{\text{mod}}$ is the theoretical model uncertainty, which is an unknown adjustable parameter.

The idea of the fit is to minimize χ^2 with the additional constraint of χ^2 per degree of freedom being equal to one. The latter condition can be obtained by adjusting the model uncertainty $\Delta \text{DE}_{\text{mod}}$, which is responsible for the spread of the theory-experiment differences. Values of model uncertainties obtained for three different Skyrme forces used in this work are collected in Table III. As it turns out, the model uncertainty is the main source of the total uncertainty, which can be checked by comparing it with the root-mean-square deviations (RMSD) between theory and experiment, see Table III.

TABLE III. Values of the model uncertainties, $\Delta \text{DE}_{\text{mod}}$, and RMSD of MDEs and TDEs obtained for three EDFs considered in this work. All values are in keV.

	SV _T	SkM*	SLy4
$\Delta \text{MDE}_{\text{mod}}$	190	150	120
RMSD(MDE)	200	150	120
$\Delta \text{TDE}_{\text{mod}}$	92	110	110
RMSD(TDE)	95	110	110

III. COMPLEMENTARY RESULTS FOR SKM* AND SLy4

As stated in the Letter, calculations of MDEs and TDEs with the extended Skyrme forces involving the strong-force class II and III contact terms were performed for three different Skyrme EDFs SV_T, SkM*, and SLy4. As shown in the Letter, within the model uncertainties, the resulting coupling constants t_0^{II} and t_0^{III} are fairly independent of the EDF. Below in Figs. 7–10, for the sake of completeness, we present results obtained for the EDFs SkM* and SLy4, whereas the analogous SV_T results were shown in Figs. 2 and 3 of the Letter. As we can see, for all three parametrizations, the agreement between experimental and theoretical values is similar. This nicely confirms that the method proposed in this work is indeed almost perfectly independent on the isoscalar charge-independent part of the functional. In this sense it is a quite robust method to assess the strong-force isospin-symmetry-breaking effects in $N \approx Z$ nuclei.

This work was supported in part by the Polish National Science Center under Contract Nos. 2014/15/N/ST2/03454 and 2015/17/N/ST2/04025, by

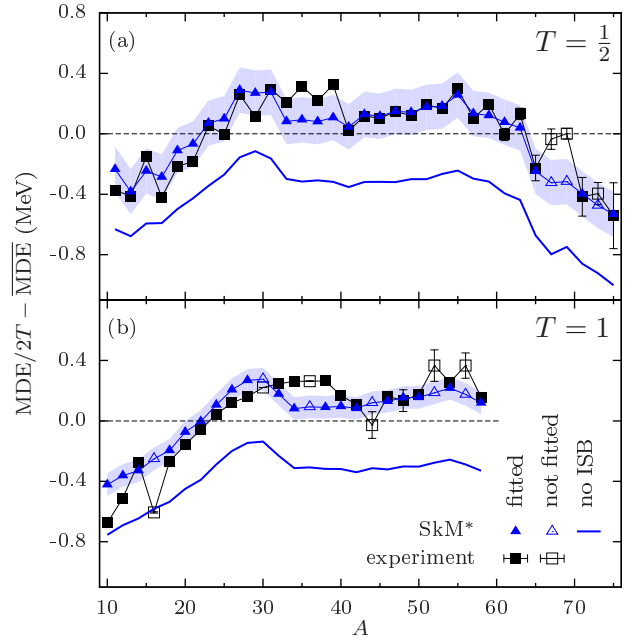


FIG. 7. (Color online) Theoretical and experimental values of MDEs for the $T = 1/2$ (a) and $T = 1$ (b) mirror nuclei, shown with respect to the average linear trend defined in Fig. 1 of the paper. Calculations were performed using SkM* functional with the ISB terms added. Shaded bands show theoretical uncertainties. Experimental error bars are shown only when they are larger than the corresponding symbols. Full (open) symbols denote data points included in (excluded from) the fitting procedure.

the Academy of Finland and University of Jyväskylä within the FIDIPRO program, by Interdisciplinary Computational Science Program in CCS, University of Tsukuba, and by ImPACT Program of Council for Science, Technology and Innovation (Cabinet Office, Government of Japan). We acknowledge the CIŚ Świerk

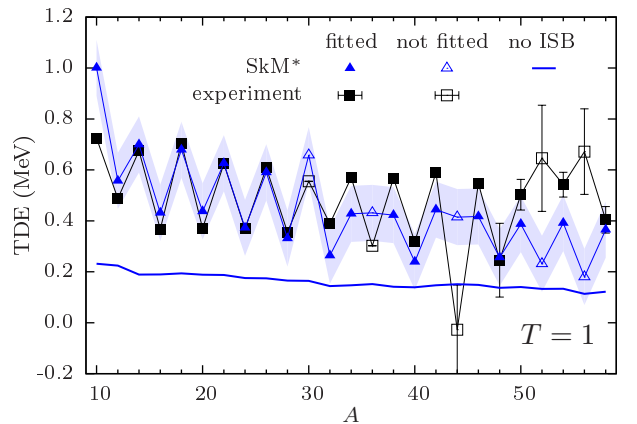


FIG. 8. (Color online) Same as in Fig. 7 but for the $T = 1$ TDEs with no linear trend subtracted.

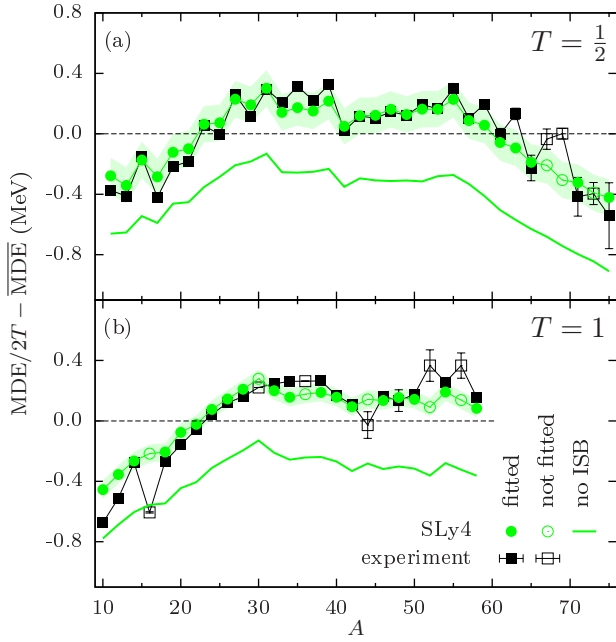


FIG. 9. (Color online) Same as in Fig. 7 but for the SLy4 EDF

Computing Center, Poland, and the CSC-IT Center for Science Ltd., Finland, for the allocation of computational resources.

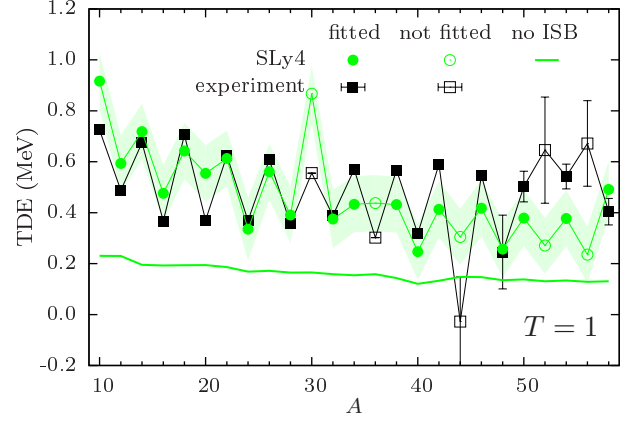


FIG. 10. (Color online) Same as in Fig. 9 but for the $T = 1$ TDEs with no linear trend subtracted.

-
- [1] J. Bartel, P. Quentin, M. Brack, C. Guet, and H.-B. Håkansson, Nucl. Phys. A **386**, 79 (1982).
 - [2] E. Chabanat, P. Bonche, P. Haensel, J. Meyer, and R. Schaeffer, Nucl. Phys. A **635**, 231 (1998).
 - [3] M. Beiner, H. Flocard, N. Van Giai, and P. Quentin, Nucl. Phys. A **238**, 29 (1975).
 - [4] W. Satuła, J. Dobaczewski, W. Nazarewicz, and M. Rafalski, Phys. Rev. Lett. **106**, 132502 (2011).
 - [5] N. Schunck, J. Dobaczewski, J. McDonnell, W. Satuła, J. Sheikh, A. Staszczak, M. Stoitsov, and P. Toivanen, Comput. Phys. Comm. **183**, 166 (2012).
 - [6] N. Schunck, J. Dobaczewski, W. Satuła, P. Bączyk, J. Dudek, Y. Gao, M. Konieczka, K. Sato, Y. Shi, X. Wang, and T. Werner, arXiv:1612.05314 [nucl-th].
 - [7] P. Bączyk, J. Dobaczewski, M. Konieczka, T. Nakatsukasa, K. Sato, and W. Satuła, arXiv:1611.01392 [nucl-th].
 - [8] W. Satuła, J. Dobaczewski, W. Nazarewicz, and T. Werner, Phys. Rev. C **86**, 054316 (2012).
 - [9] P. Bączyk, J. Dobaczewski, M. Konieczka, and W. Satuła, Acta Phys. Pol. B Proc. Supp. **8**, 539 (2016).
 - [10] J. Dobaczewski, W. Nazarewicz, and P.-G. Reinhard, J. Phys. G: Nucl. Part. Phys. **41**, 074001 (2014).
 - [11] M. Wang, G. Audi, A. H. Wapstra, F. G. Kondev, M. MacCormick, X. Xu, and B. Pfeiffer, Chin. Phys. C **36**, 1603 (2012).
 - [12] Evaluated Nuclear Structure Data File, <http://www.nndc.bnl.gov/ensdf/>.